Supporting Information for

Structural Analysis of the Effect of a Dual-FLAG Tag on Transthyretin

Mehdi Shirzadeh, Michael L. Poltash, Arthur Laganowsky and David H. Russell*
Department of Chemistry, Texas A&M University, College Station, Texas 77843

*Corresponding author: russell@chem.tamu.edu

Table of Contents

Mass and charge effect on CIU and VT-ESI results

To take account of mass variation for each protein, the CIU energies required for unfolding of N to I_1 are normalized. Also, ion charge can affect the energy requirement for unfolding *i.e.* more energy is required to unfold lower charge state ions. Thus, to cancel the effect of charge state on the stability analysis we plotted the resulting charge states from AA and charge reduced solution using TEAA. Surprisingly, despite the mass differences, WT- and CT-TTR unfold at similar energy per mass, and at charge zero (z=0) they require nearly the same energy per mass, *i.e.* 2.59 and 2.72 V/kDa, respectively. A non-linear correlation between charge and normalized energy was obtained for FT_2-TTR, and with the best fit possible, at z=0, a relatively high energy is required for unfolding the N conformer (58.3 V/kDa). Taken together, CIU experiments reveal the utility of IM-MS to screen and assess structural changes introduced *via* purification tags in gas phase.

Origin of metal-induced oxidation

We have discovered previously[1] that metals such as copper and chromium, but not zinc, induce Cys10 oxidation; thus, added thermo-cleaved peptide can enhance the oxidation rate of WT-TTR in two different ways: (i) removing the endogenous zinc bound to WT-TTR, and/or (ii) providing excess copper for TTR oxidation. The mass spectrum of the isolated thermo-cleaved peptide reveals a binding species (~63 Da), which is most likely the copper metal as we measured a higher affinity towards copper compared to zinc (**Figure S10**). Accurate assignment of which metal is bound to peptide was not possible due to overlapping in the theoretical mass spectra of thermo-cleaved peptide bound to Cu and Zn (**Figure S11**). In our previous study, several metals were detected in WT-TTR solution using ICP-MS and copper was the third most abundant metal in solution.[1] Preferential binding towards copper has been previously reported for poly-aspartic

acid polymers which has sequence similarity to FT_2 tag.[2, 3] Thus, we attributed oxidation of WT-TTR in the presence of thermo-cleaved peptide to an increase in copper concentration in which thermo-cleaved peptide can exchange its copper with WT-TTR. To conform this hypothesis, the isolated thermo-cleaved peptide was incubated with 2mM DTPA for 5 h at 24 °C followed by elution of excess DTPA using Ziptip. The peak with 63 Da shift was no longer observed in the mass spectrum indicating the complete removal of copper. Incubation of the resulting metal-free peptide with WT-TTR completely eliminated the metal-induced oxidation.

Table S1. Instrument parameters (Synapt G2, Waters) used in native MS analysis.

capillary voltage (kV)	*sampling cone (V)*	*trap gas (Ar) flow (L.min^{-1})*	*He flow (L.min^{-1})*	*IM gas (N_2) flow (L.min^{-1})*	*trap DC bias*
1.0-1.5	20	4	120	60	40

Table S2. First intermediate in FT_2-TTR unfolding is structurally different than WT- and CT-TTR. CCS values of native (N), intermediates (I_1, I_2, I_3) and unfolded (U) conformers of TTR variants upon gas phase unfolding. With discarding I_1 as the first intermediate for FT_2-TTR, a good match in changes of CCS values of intermediates for all three proteins is obtained.

	N (Å^2)	*I_1 (Å^2)*	*I_2 (Å^2)*	*U (Å^2)*	*I_3 (Å^2)*	*I_1/N*	*I_2/N*	*U/N*	*norm (i/wt)*	*norm (i/wt)*	*norm (i/wt)*
WT	3864	5044	5576	6143		1.305	1.443	1.590	1	1	1
CT	3968	5128	5690	6178		1.292	1.434	1.557	0.990	0.994	0.979
FT_2	4018	4913	5210		5806	1.223	1.297	1.445	**0.937**	**0.899**	**0.909**
FT_2	4018	5210	5806	5994		1.297	1.445	1.492	**0.993**	**1.001**	**0.938**

Table S3. Standard error calculation of VT-ESI measurements at 25 °C. Measurements at each temperature (25, 42, 62 and 78 °C) were repeated three times with different samples on different days (i.e. rep 2 was collected 9 month after rep 1). Note the error obtained for FT_2-TTR at 78 °C.

	rep1	*rep2*	*rep3*	*mean*	*s.d.*	*%s.d.*
WT (25 °C)	45.70	45.02	44.78	45.17	0.39	0.87
CT (25 °C)	48.58	50.25	49.58	49.47	0.69	1.39
FT_2 (25 °C)	56.11	61.84	64.63	60.86	3.57	5.83
FT_2 (78 °C)	22.15	56.84	63.82	47.60	18.22	38.29

Table S4. Top-down analysis of thermo-cleaved peptide (4+) and corresponding fragments. Data is only shown for 1+ fragments.

	experiment	*theoretical*	*ppm*		*experiment*	*theoretical*	*ppm*
y2	234.1435	234.1448	5.5521	***b2***	260.0883	260.0877	2.3070
y3	363.1888	363.1874	3.8548	***b3***	423.1504	423.1510	1.4179
y4	420.2062	420.2089	6.4254	***b4***	551.2443	551.2460	3.0839
y5	521.2542	521.2566	4.6042	***b5***	666.2803	666.2729	11.1066
y6	578.2723	578.2780	9.8569	***b6***	781.2975	781.2999	3.0718
y7	679.3306	679.3257	7.2130	***b7***	896.3233	896.3268	3.9048
y8	776.3813	776.3785	3.6065	***b8***	1011.3476	1011.3538	6.1304
y9	833.3945	833.3990	5.3996	***b9***	1139.4585	1139.4487	8.6006
y10	961.5015	961.4949	6.8643	***b10***	1254.4684	1254.4757	5.8192
y11	1076.5340	1076.5218	11.5186	***b11***	1417.5392	1417.5390	0.1411
y12	1191.5370	1191.5488	9.7352	***b12***	1545.6188	1545.6340	9.8341
y13	1306.5540	1306.5757	16.3787	***b13***	1660.6416	1660.6609	11.6219
y14	1421.5910	1421.6027	8.4412	***b14***	1775.6821	1775.6879	3.2663
y15	1549.6260	1549.6976	46.5252	***b15***	1890.6956	1890.7148	10.1549
y16	1712.7020	1712.7610	34.5641	**-**			
y17	1827.7820	1827.7879	3.1732	**-**			

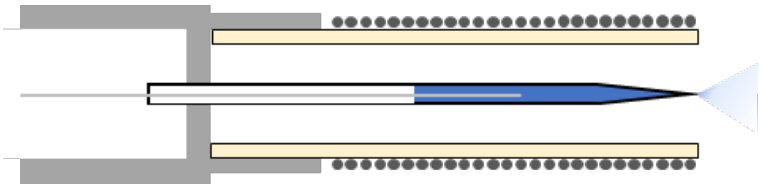

Figure S1. Schematic of developed ESI source for varying the solution temperature. Kantal wire is resistively heated with change in DC current. A ceramic spacer is used to isolate electric current from emitter and transfer heat evenly distributed. Pt wire is used to apply current to solution for ESI.

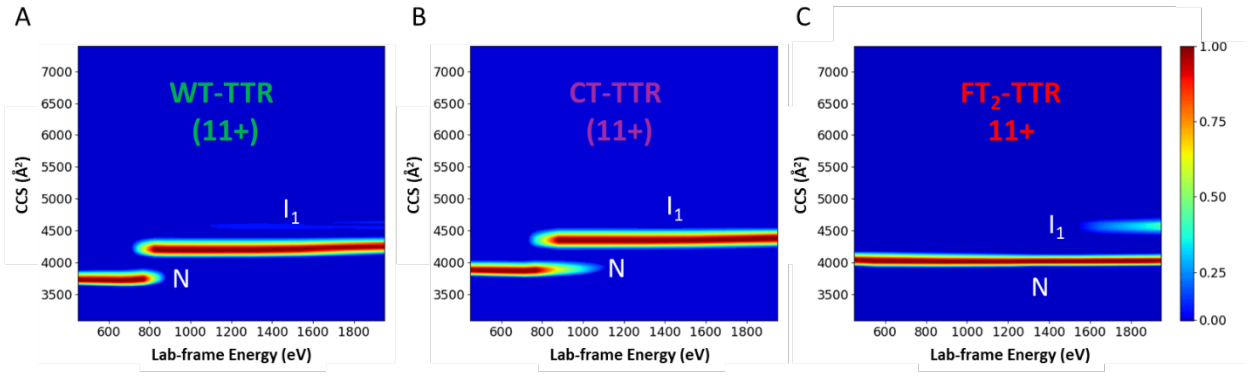

Figure S2. CIU plots of (A) WT-TTR and (B) CT-TTR (C) FT_2-TTR (11+). Charge reduction of TTRs reveals the differences in gas-phase stabilities of WT- vs FT_2-TTR where the latter remains as native conformer at ~1900 eV, whereas two others undergo unfolding to first intermediate at ~800 and 870 eV (WT- and CT- respectively).

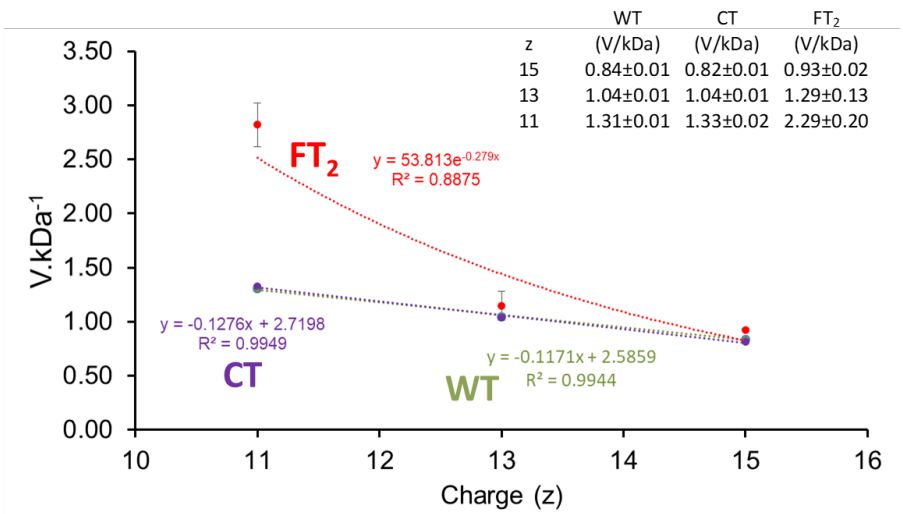

Figure S3. Normalized energies for unfolding the native conformer to the first intermediate for ions with three different charges (11+, 13+ and 15+). WT- and CT- demonstrate linear trend and very close unfolding energy per mass (for z=0, 2.59, 2.72 V.kDa^{-1} respectively). FT_2-TTR, however, shows non-linear trend and higher stability in gas-phase at each charge states and 58.3 V.kDa^{-1} for z=0.

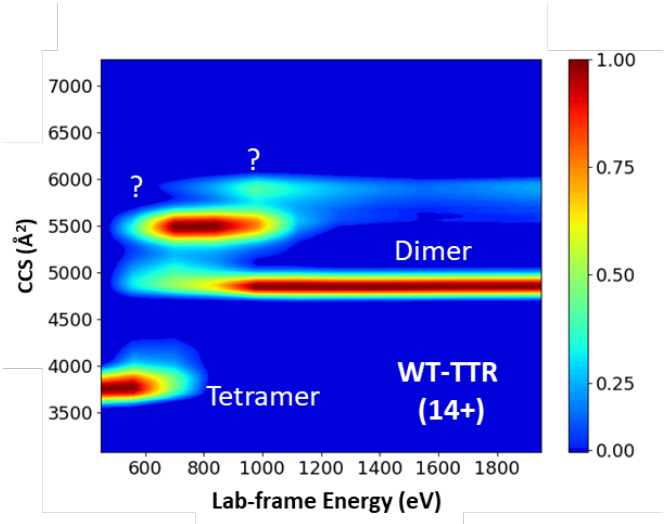

Figure S4. Overlapping unfolding signal with the evenly charged tetramer and dimer signals. CIU plot of WT-TTR in 200 mM ammonium acetate (14+).

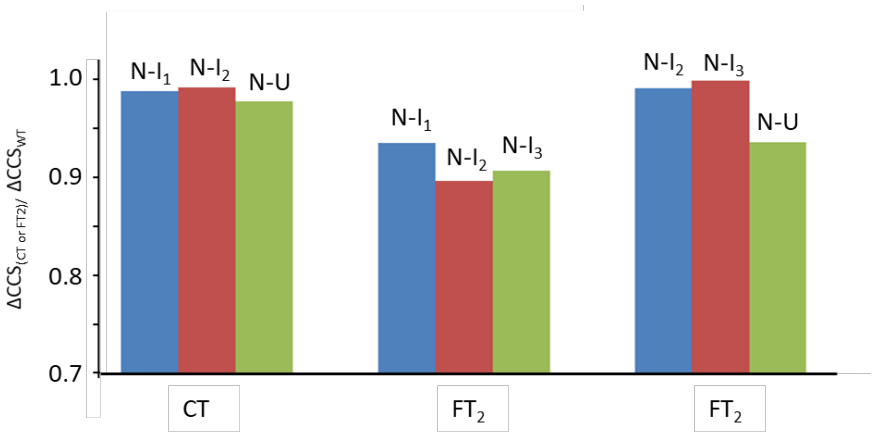

Figure S5. Plot obtained from Table S4. This plot obtained from three last columns in Table S4 showing the better correlation of unfolding transition after discarding the first intermediate of FT_2-TTR.

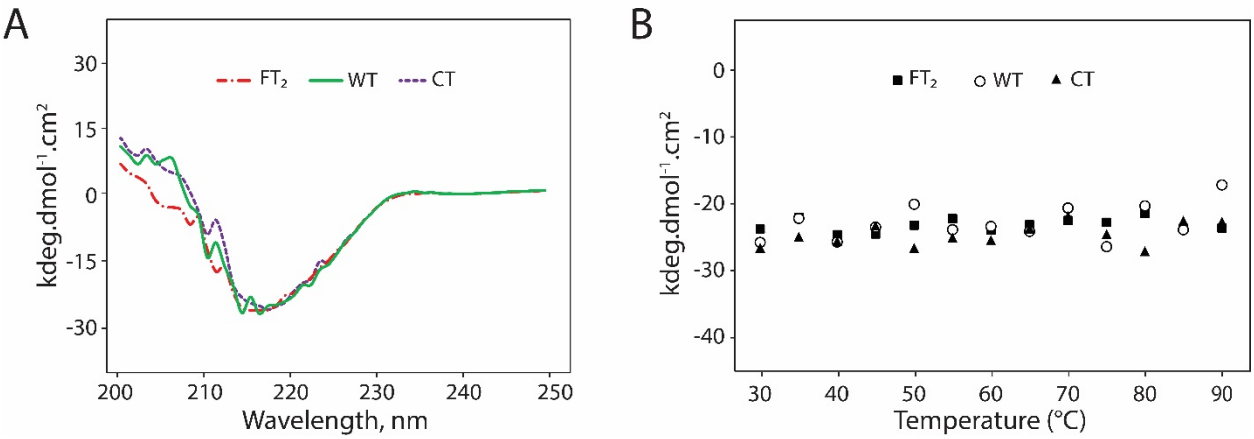

Figure S6. Secondary structure analysis and melting temperature measurement of TTR variants. (A) CD spectra of WT-TTR (green, solid line), CT-TTR (purple, dashed line) and FT_2-TTR (red, dot dashed line) in 10 mM Na_2HPO_4, pH 7.4 at room temperature. (B) Thermal stability measurement (at 220 nm) in 10 mM Na_2HPO_4, pH 7.4.

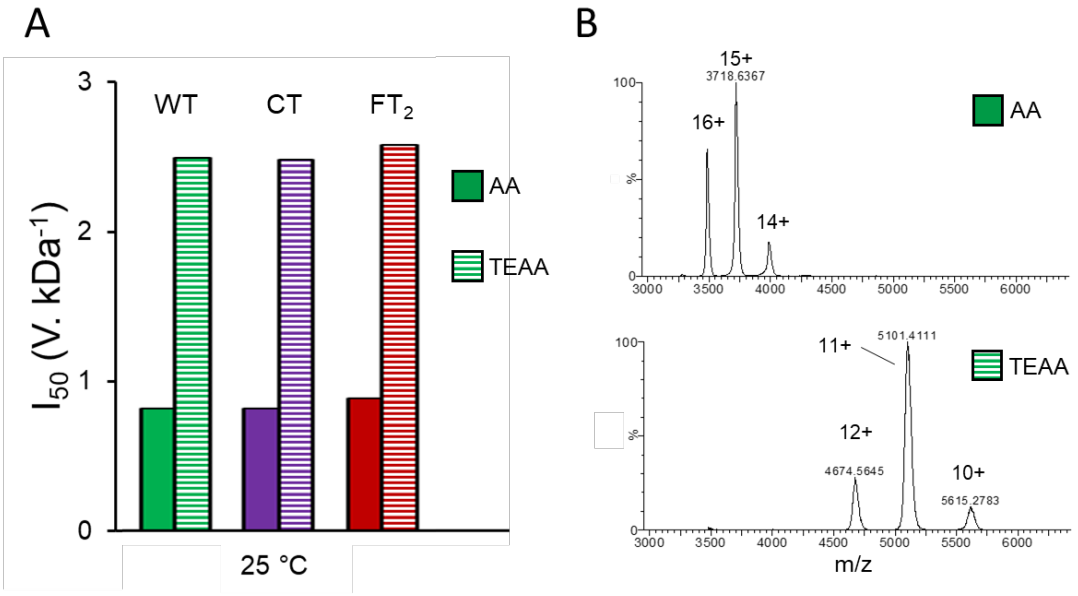

Figure S7. Charge effect on energy required for dissociation of TTR samples. (A) Plot of normalized I_{50} (V.kDa^{-1}) for solution electrosprayed from conventional buffer used in native MS, AA, (14+, 15+ and 16+) and charge reduced by TEAA (10+, 11+ and 12+). (B) Corresponding mass spectra for WT at 25 °C.

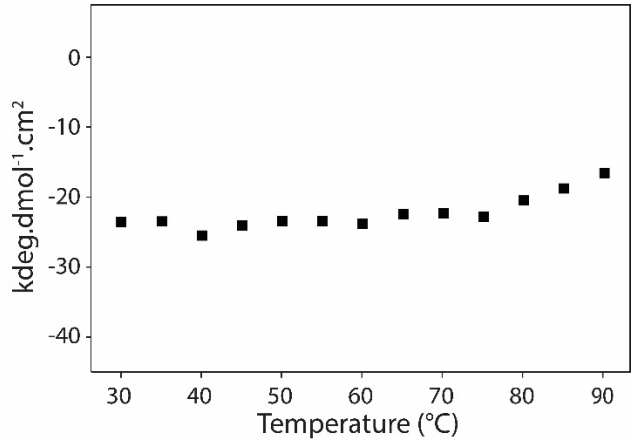

Figure S8. Poor reproducibility of FT_2-TTR melting point experiments using CD spectroscopy. Some FT2-TTR samples show unfolding at high temperatures (70 °C<).

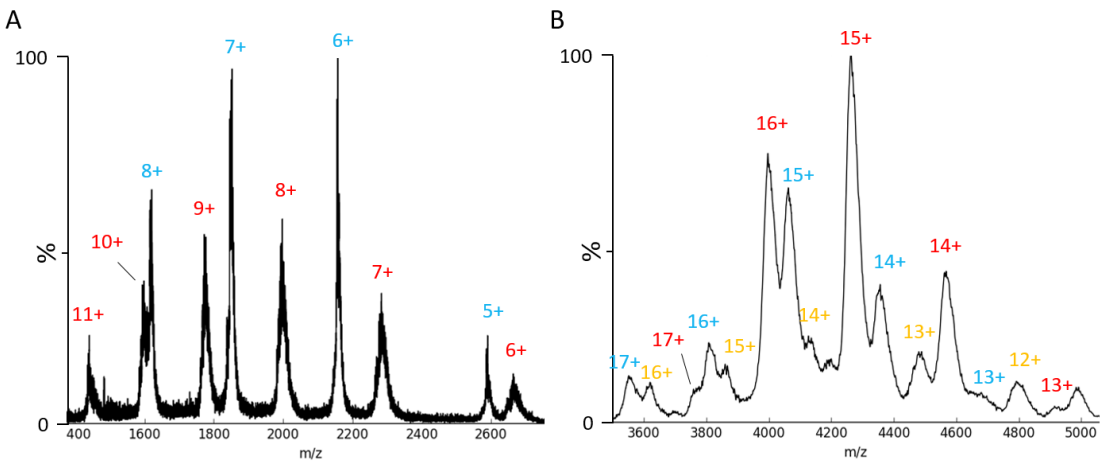

Figure S9. Truncated monomer is ejected with gas-phase activation of thermally treated FT_2-TTR (A) Monomeric ions (red=intact and cyan=truncated) (B) and tetrameric ions (red=intact, cyan=with one truncated subunit and yellow= with two truncated subunits) resulted from collision-induced dissociation of FT_2-TTR incubated at 50 °C for 18 h.

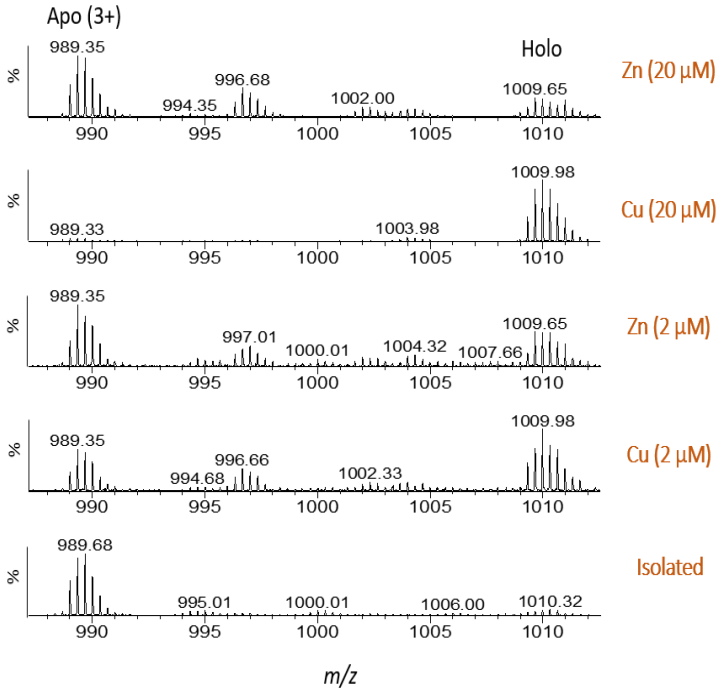

Figure S10. Mass spectra of thermo-cleaved peptide binding to copper and zinc. The bottom spectrum is for the isolated peptide after reconstitution into 200 mM ammonium acetate. Apo signal almost disappeared from solutions with added 20 µM copper, unlike zinc which has relatively similar ratio of apo:holo in solutions with 2 µM and 20 µM zinc acetate.

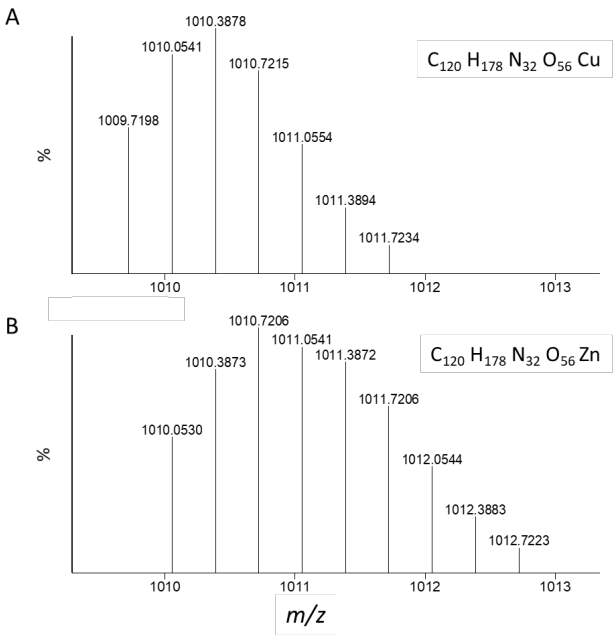

Figure S11. Theoretical mass spectra of thermo-cleaved peptide $(M+3H)^{3+}$bound to (A) Cu (II), (B) Zn (II). Overlapping MS spectra of the peptide bound to Cu or Zn prevents accurate assignment of experimental data.

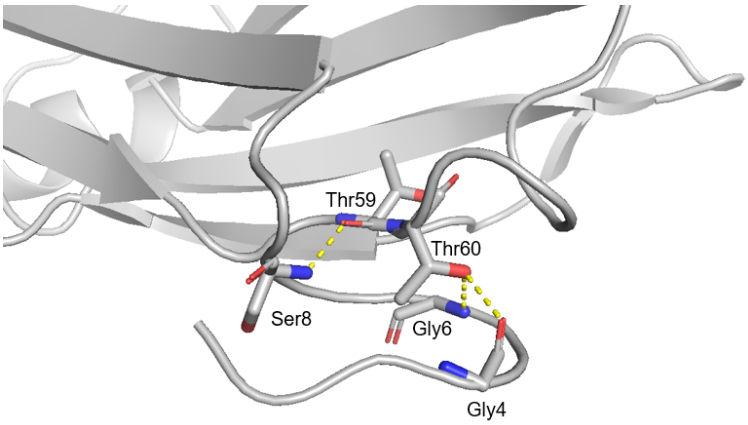

Figure S12. N-terminal domain of TTR interacts with protein backbone. Hydrogen bond between Thr59 and Glu7 showing interaction of N-terminus and backbone of TTR. Pymol is used to generate and render the image using crystal structure of TTR mutants, V30M (PDB 1ttc).

References

1. Poltash, M.L., et al., *New insights into the metal-induced oxidative degradation pathways of transthyretin.* Chem Commun (Camb), 2019. **55**(28): p. 4091-4094.
2. Thombre, S.M. and B.D. Sarwade, *Synthesis and Biodegradability of Polyaspartic Acid: A Critical Review.* Journal of Macromolecular Science, Part A, 2005. **42**(9): p. 1299-1315.
3. Kołodyńska, D., Z. Hubicki, and M. Gęca, *Polyaspartic Acid As a New Complexing Agent in Removal of Heavy Metal Ions on Polystyrene Anion Exchangers.* Industrial & Engineering Chemistry Research, 2008. **47**(16): p. 6221-6227.